

Water Resources Research®



RESEARCH ARTICLE

10.1029/2023WR034994

Comparing Agriculture-Related Characteristics of Flash and Normal Drought Reveals Heterogeneous Crop Response

Sarah Ho^{1,2} , Allan Buras³, and Ye Tuo² 

¹Karlsruhe Institute for Technology, Institute of Water and River Basin Management - Hydrology, Karlsruhe, Germany, ²Technical University of Munich, School of Engineering and Design, Chair of Hydrology and River Basin Management, Munich, Germany, ³Technical University of Munich, School of Life Sciences, Professorship for Land Surface-Atmosphere Interactions, Munich, Germany

Key Points:

- Flash droughts exhibit significantly different spatial distributions and trends in characteristics than normal droughts
- Aridity can provide useful clues about vegetation condition and irrigation's effectiveness during drought
- Flash drought conditions (temperature and radiation) may alleviate plant growth limitations in cooler climates, improving vegetation condition

Supporting Information:

Supporting Information may be found in the online version of this article.

Correspondence to:

S. Ho,
sarah.ho@kit.edu

Citation:

Ho, S., Buras, A., & Tuo, Y. (2023). Comparing agriculture-related characteristics of flash and normal drought reveals heterogeneous crop response. *Water Resources Research*, 59, e2023WR034994. <https://doi.org/10.1029/2023WR034994>

Received 31 MAR 2023

Accepted 3 NOV 2023

Author Contributions:

Conceptualization: Ye Tuo
Formal analysis: Allan Buras
Investigation: Allan Buras, Ye Tuo
Supervision: Ye Tuo
Writing – review & editing: Allan Buras, Ye Tuo

Abstract Despite rapid progress in the burgeoning field of flash drought research, few studies directly compare the differences in characteristics between flash drought (commonly understood as quick, rapid-onset drought) and drought traditionally defined as slow-moving (henceforth normal drought), particularly over agricultural regions where drought effects may be economically the most disastrous. In this study, flash and normal drought events are identified using reanalysis of soil moisture in the data-rich agricultural region of the California Central Valley for investigation of characteristics related to agriculture. In particular, we investigate the relative duration of pixels in drought events, the correlation of drought intensity with vegetation condition, the impact of aridity on vegetation response and drought, and the differences in the different characteristics between rainfed and irrigated agriculture. Overall, we found considerable differences between flash and normal drought, particularly in their spatial distributions and behavior in relation to aridity. Flash droughts even indicate a counterintuitive improvement in vegetation condition in the northern, more humid regions, likely due to the release of growth limiting factors (e.g., below-optimum temperature and radiation) associated with drought. Results also indicate improvements in vegetation conditions during normal drought for irrigated land over rainfed, highlighting the importance of irrigation as a drought protection strategy in agriculture.

Plain Language Summary Flash droughts are droughts that, in contrast to traditionally understood droughts, develop suddenly and rapidly. This can be particularly dangerous for agriculture, since crops can be affected by sudden changes in plant available water. This study identifies differences in drought characteristics over the Central Valley agricultural region of California, such as length of time in drought and effects on vegetation, with considerations for local climate and irrigation. Overall, flash drought shows clear spatial trends that vary with local climate, with some regions showing a benefit to plant health during flash droughts, and irrigated regions performing slightly better. This highlights the importance of irrigation as an adaptation strategy against drought.

1. Introduction

Within the widely recognized phenomenon of drought is the recently recognized phenomenon of flash drought. This term describes a subset of drought on a sub-seasonal (weeks to months) scale commonly characterized by rapid intensification (Noguera et al., 2021; Osman et al., 2021; Otkin et al., 2018; Pendergrass et al., 2020). While normal drought has typically been defined by rainfall deficits (among other water shortages, depending on the drought type—for example, streamflow for hydrological and soil moisture for agricultural drought), many approaches to identifying flash drought are based on changes in evapotranspiration (ET) and soil moisture (Chen et al., 2019; J. Li, Wang, Wu, et al., 2020; Liu et al., 2020; Nguyen et al., 2019; Otkin et al., 2018; Otkin et al., 2016; Wang & Yuan, 2018; X. Xiao et al., 2019). Despite the recent uptick in research on its identification and propagation, much is still unknown about flash drought.

The identification of flash drought events is, similar to its normal counterpart, a developing field. The subjectivity of drought definitions remains a significant barrier to a universally applicable definition (Guo, Bao, Liu, et al., 2018; Guo, Bao, Ndayisaba, et al., 2018; Sheffield et al., 2009; Spinoni et al., 2019; Zang et al., 2019), though some may argue that such a definition is unnecessary, stressing a functional (rather than theoretical) definition (Lloyd-Hughes, 2013). Functional definitions have since been postulated for flash drought, focusing on two aspects: first, that there is a rapid intensification of water deficits; and second, that the deficit reaches drought

© 2023. The Authors.

This is an open access article under the terms of the [Creative Commons Attribution License](https://creativecommons.org/licenses/by/4.0/), which permits use, distribution and reproduction in any medium, provided the original work is properly cited.

conditions (Otkin et al., 2018). Several methods now exist that define flash drought based on soil moisture or evaporation conditions, as these have been shown to be most closely linked with flash drought (Chen et al., 2019; Ford et al., 2015; Ford & Labosier, 2017).

In their review of flash drought literature, Otkin et al. (2018) called for researchers to unite under a singular definition of flash drought as a subset of drought characterized by a high rate of intensification rather than a short duration. Such definitions can be expressed in a rate-of-change relationship involving a change in severity over time. An example is that of Chen et al. (2019), where flash droughts are explicitly defined by areas that, in a 4-week period, experience a two-category change in dryness in the U.S. Drought Monitor. Pendergrass et al. (2020) refine this definition by imposing criteria that the two-category change must happen over the course of 2 weeks and maintain that change for another two. They also proposed a definition for international usage based on a 50% increase in the evaporative demand drought index (EDDI) over 2 weeks and sustained for another two. Similar intensification approaches in soil moisture are used by Liu et al. (2020). However, many of these definitions are constrained to a single area and may not be able to capture how drought moves and expands over time. J. Li, Wang, Wu, et al. (2020)'s use rate-of-change principles created criteria that account for both intensity and area, but also still employed a short-duration filter. This allows the identification of flash drought with potential for global use that includes their movement in space and time, which is useful for analyzing flash drought and its effects over different land and vegetation types.

A particular concern for flash drought is its effect on agriculture, as previous studies have clearly illustrated normal drought's detrimental impacts to vegetation (Dong et al., 2019; Guo, Bao, Ndayisaba, et al., 2018; Ji & Peters, 2003; W. Li et al., 2022; Nicolai-Shaw et al., 2017; Vicente-Serrano et al., 2013). While Zhang and Yuan (2020) found that crops do show rapid reactions to flash drought, their comparative analysis between biomes did not allow for spatial heterogeneity within crop regions—for example, how irrigation or soil texture can impact these findings.

The advent of widely available, high-quality remote sensing products has been a boon for drought research, particularly with regard to spatial detail. For example, the Normalized Difference Vegetation Index (NDVI) has been commonly used in drought monitoring as a proxy for plant health (Dong et al., 2019; Gillespie et al., 2018; Goldberg et al., 2010; Gu et al., 2007; Ji & Peters, 2003). The impacts of drought on vegetation have been shown to be related to local dryness, also known as aridity, which can be calculated using long-term remote sensing products. While similar to drought in that they both express dryness, aridity is a descriptor of conditions without reference to typical levels—a key component of drought (Le Houerou, 1996)—and is typically calculated over longer periods of time (Zomer & Trabucco, 2022), making it a useful baseline for comparison between areas. Other studies, such as Orth et al. (2020) and O and Park (2023), found that vegetation health indicators vary with aridity—in particular, that arid regions show strong responses and humid regions show weak ones—and that they intensify with increasing drought duration. This is consistent with Vicente-Serrano et al. (2013), who found that regions with different aridity tend to respond to drought at different time scales, with arid regions responding faster than humid ones. They also hypothesize that this may be due, in part, to differing adaptation strategies in local plants, which is corroborated by Buras et al. (2020). A potential explanation for this behavior is that, despite a large relative anomaly suggested by standardized indicators, actual water deficit conditions may not be severe enough to result in actual damage, particularly in typically cool and moist regions (Zang et al., 2019). However, these flash drought studies lack specific investigation into agricultural regions, which are significantly more managed. Whether these patterns of vegetation response based on aridity and duration still hold in significantly shorter flash drought events, particularly for agriculture, needs still more investigation.

As extreme events become more frequent due to changing climate, it becomes critical to investigate flash drought and its effects on agriculture and food production. A frequency study of flash drought over the conterminous United States found that, although the drought-stricken state of California experiences fewer flash droughts than the rest of the country, the Central Valley region—an agricultural powerhouse—still experiences extreme flash drought approximately every 5–6 years (X. Xiao et al., 2019). Given the strong dependence on groundwater withdrawal for irrigation in the region threatening local aquifers (Cody et al., 2015; Pauloo et al., 2020; Wilson et al., 2016; M. Xiao et al., 2017), the degree of impact that irrigation has in tempering adverse drought effects—particularly in flash drought, for which little research exists—should be investigated.

In this study, the differences in agriculture-related characteristics of soil moisture drought—namely the relationships between the NDVI-soil moisture correlation and relative duration of drought—and their variations with

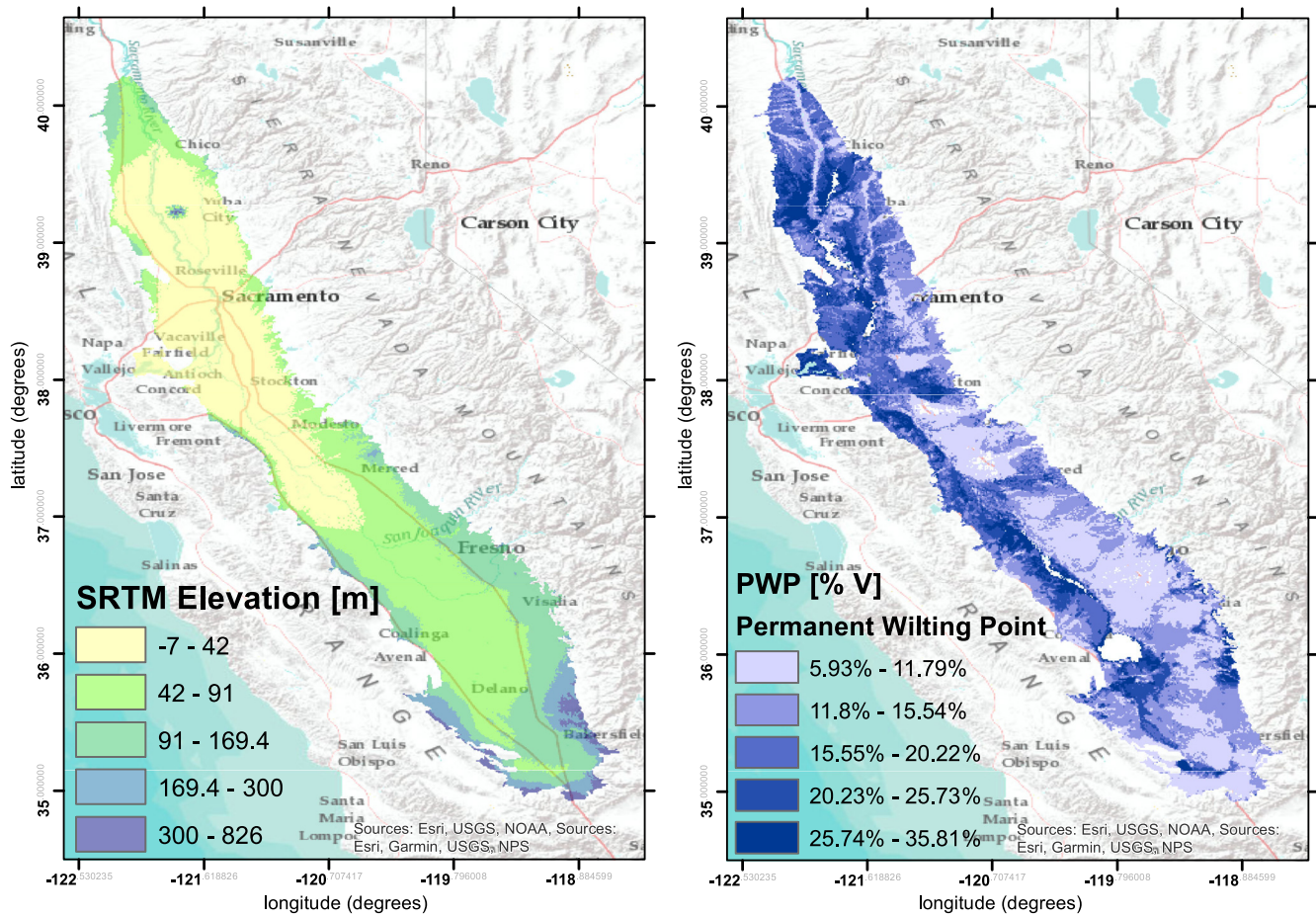


Figure 1. Elevation map (left) of the study area (California Central Valley, USEPA Ecoregion 7), generated using SRTM (NASA-JPL, 2013), and permanent wilting point (PWP) as volumetric soil water content (right), calculated using soil data from the California Soil Resource Lab (Walkinshaw et al., 2022), according to Saxton et al. (1986).

aridity and irrigation are compared between the shorter, faster onset flash drought events and normal drought events in the data-rich and drought-prone region of the California Central Valley. In particular, we focus on the following hypotheses (referenced throughout the study as H1, H2, and H3).

- H1: Longer duration of normal drought will result in more spatially homogeneous drought characteristics and more negative impacts on vegetation in comparison to flash drought. As a corollary, regions spending relatively longer time per event in a particular drought type will experience stronger changes in vegetation response.
- H2: The aridity of a region strongly impacts the agricultural vegetation response of a region to drought. More specifically, agriculture in humid regions may benefit short-term from flash drought events because the anomaly indicated by a standardized index (SI) does not correspond to a true plant water deficit.
- H3: Irrigation will provide a tempering effect on adverse vegetation responses to both flash and normal drought, independent of aridity.

2. Study Area

The California Central Valley is a level three ecoregion as defined by the United States Environmental Protection Agency (Griffith et al., 2016) encompassing approximately 47,000 km², or roughly 10% of the state's total area (Figure 1). It is a stretch of flat plains bordered by coastal mountains to the west and the Sierra Nevada mountain range to the east. Over half of the ecoregion is classified as farmland, which is farmed intensively throughout the year (Griffith et al., 2016; Teluguntla et al., 2015). The mild climate, along with loamy soils with low wilting

points (Figure 1) favorable for agriculture (Walkinshaw et al., 2022), makes it one of the largest, most productive agricultural regions in the United States with exports all over the world (Marston & Konar, 2017).

Permanent wilting point (PWP) is used in this study as a simplified proxy for soil texture that also communicates the minimum volume of water necessary to maintain plant life. PWP values for the region were calculated using soil texture data from the California Soil Resource Lab (Walkinshaw et al., 2022), according to Saxton et al. (1986) and can be seen in Figure 1.

However, the region—as with much of the state—is subject to frequent and intense droughts. It exists in a climatic transition zone (Dong et al., 2019): while overall, the region is semiarid and heavily dependent on irrigation, particularly groundwater (Cody et al., 2015), the northern half of the area is generally cooler and wetter than the southern part. Several studies have indicated a drying trend in California, particularly in the southern region (Dong et al., 2019; Okin et al., 2018).

The recent 2011–2017 drought that peaked in 2014 is considered among the most intense and severe in recent history (Dong et al., 2019; Erlingis et al., 2021; Griffin & Anchukaitis, 2014; Lund et al., 2018; M. Xiao et al., 2017), resulting in heavy aquifer withdrawals that resulted in soil subsidence (Cody et al., 2015; M. Xiao et al., 2017). As this is a long and extremely severe drought event that is well-documented as an extraordinarily impactful slow-moving drought, this study will focus on available data through 2012. Soil moisture drought indices and drought identification encompass the years 1980–2012, while the vegetation condition-related analyses focus on the years 2000–2012.

3. Data and Methods

3.1. Drought and Flash Drought Identification

While a pixel-by-pixel-based analysis can be useful for understanding drought dynamics in specific locations, drought identification methods that study its movement within a catchment are useful for understanding regional spatial patterns. This work applies the methodology of J. Li, Wang, Wu, et al. (2020) for identifying and tracking flash droughts for the study area with some slight modifications. Though the originally developed for use with the Standardized Evaporative Deficit Index (Vicente-Serrano et al., 2018), the method should be applicable to any SI. In brief, the method (with modifications) is as follows (J. Li, Wang, Wu, et al., 2020).

1. *Identification of drought patches (clusters)* above an area threshold using a chosen drought index calculated on a 5-day timescale. The area threshold, according to the method, is 1.6% of the study area (in this case, roughly 750 km²), and the drought index used is the Standardized Soil Moisture Index (SSmI) (AghaKouchak, 2014; Hao & AghaKouchak, 2013) calculated on a 5-day scale for every available time step. To be part of a cluster, a pixel must
 - a. have an SI value of less than or equal to -1 (threshold dryness)
 - b. be adjacent to another pixel with $SI < -1$ in the cluster

The 1.6% area threshold and 5-day timescale are parameters selected by the original authors of the method. The 1.6% area threshold has been used often in other spatial analyses of drought (Guo, Bao, Liu, et al., 2018; Ho et al., 2021; J. Li, Wang, & Lai, 2020; Xu et al., 2015), which was the proportion of area found by Wang et al. (2011) to be most sufficient for preventing tenuous spatial connectivity. The 5-day (i.e., pentad) time scale has also been commonly used in other flash drought identification methods (Christian et al., 2019; Ford & Labosier, 2017; Mo & Lettenmaier, 2015; Wang & Yuan, 2018).
2. *Checking spatial connection of drought clusters.* This step helps ensure that two clusters are continuous in time and meaningfully connected in space (i.e., they are part of the same drought event). The spatial connection between two clusters in consecutive timesteps is verified by the conditions that they must be
 - a. more than 50% of the area of the smaller drought cluster, and
 - b. more than the minimum drought cluster area threshold (1.6% of the study area).
3. *Elimination of connected clusters lasting less than a total of five pentads (25 days).* In this work, all remaining collections of clusters after this step are considered drought events. Subsequent steps are used to differentiate flash droughts from normal droughts.
4. *Division of the event into development and recovery phases.* This is done using the rate of change of the drought intensity of the whole cluster or patch (drought patch intensity DPI), for each time step k

$$DPI_k = \sum_{i=1}^n SI \quad (1)$$

where SI is the value of the standardized drought index (in this case $SSmI$) for a particular point and n is the number of pixels in the drought patch. The timestep with the most negative value of DPI is considered the peak intensity; all timesteps before the peak are the development period and all timesteps after are the recovery period. Based on this definition, similar DPI values may refer to either severe droughts on small scale as well as moderate droughts on large scale. While actual effects will differ between these scenarios, from a water managers' standpoint the consequences will be relatively similar.

5. *Calculation of the instantaneous intensification rate (IIR) and the average IIR (AIIR).* The IIR is based on the change of DPI , referred to as the cumulative standardized value (CSV):

$$CSV_k = DPI_{k+1} - DPI_k \quad (2)$$

The change in CSV for each time step, adjusted for grid size by dividing by the total number of pixels n involved in each drought patch, is calculated as

$$\overline{\Delta CSV}_{k,k+1} = \frac{CSV_{k+1} - CSV_k}{n_{k,k+1}} \quad (3)$$

The IIR is then the division of the change in CSV by the difference in time steps t :

$$IIR_{k,k+1} = \frac{\overline{\Delta CSV}_{k,k+1}}{t_{k+1} - t_k} = \frac{1}{t_{k+1} - t_k} \left(\frac{DPI_{k+2} - 2DPI_{k+1} + DPI_k}{n_{k,k+1}} \right) \quad (4)$$

Given this forward calculation, it follows that the calculation of IIR—and by extension, AIIR—is only possible for $m - 2$ timesteps, where m is the total number of timesteps in the drought event. Thus, the average IIR (AIIR) is calculated as the average values of the IIR for $m - 2$ timesteps during the flash drought development period (i.e., until the peak of drought) only,

$$AIIR = \frac{\sum_{i=1}^{m-2} IIR_{k,k+1}}{m} \quad (5)$$

It should be noted that these equations here assume intensification, that is, that IIR and AIIR will be negative. If they are positive, this indicates a recovery rate, and are identified by J. Li, Wang, Wu, et al. (2020) as an instantaneous recovery rate (IRR) and average IRR (AIRR).

6. *Identification of flash drought events.* To be considered a flash drought event, the event must fulfill all the following criteria:
- The duration of the event lasts longer than five pentads (25 days);
 - The duration of the event may not exceed 12 pentads (60 days); and
 - The AIIR is more negative than or equal to the 45th percentile of the cumulative distribution frequency of ΔCSV during the development phase.

Drought events that satisfy *a* but fail *b* and/or *c* are considered traditional or normal drought events.

This work has modified J. Li, Wang, Wu, et al. (2020)'s method in four ways. First, the use of $SSmI$ rather than $SEDI$ was driven by a preliminary study that showed significantly more homogeneity in $SEDI$ than $SSmI$. Second, the omission of a pixel buffer as originally suggested is due to the higher resolution of the $WLDAS$ data set (0.01° vs. 0.25°) eliminating the need for a pixel buffer to capture potential edge effects. Third, the change in AIIR condition from the 40th in the original method to the 45th as used here was driven by sensitivity analysis in the region (for more, see Figure S1 in Supporting Information S1). Finally, a criterion in the original study proposed that one or more IIRs should exist that are less than or equal to the 25th percentile of the cumulative distribution frequency of ΔCSV during the development phase; however, because this study calculated the 5-day $SSmI$ on a daily timestep (i.e., for every day, there is an $SSmI$ value calculated using the previous 5 days), the ΔCSV and IIR are equivalent:

$$IIR_{k,k+1} = \frac{\overline{\Delta CSV}_{k,k+1}}{t_{k+1} - t_k} = \frac{\overline{\Delta CSV}_{k,k+1}}{1} = \overline{\Delta CSV}_{k,k+1} \quad (6)$$

Thus, there is always guaranteed to be one IIR that is less than or equal to the 25th percentile of Δ CSV. The additional criterion is therefore superfluous and has been omitted. A brief exploration of how the changed scale and criteria can be found in Figure S2 of Supporting Information S1. For further details on the method, we refer to Figures 1 and 2 in the original method paper by J. Li, Wang, Wu, et al. (2020).

It is important to note that this definition of flash drought is significantly more stringent on duration than most contemporary definitions. Whereas most definitions require an end in drought conditions within a designated development period (for which the consensus, according to Lisonbee et al. (2021), is within 40 days), thus emphasizing a rapid onset, this definition requires that a drought event develops and terminates within 60 days. However, other aspects of this definition—namely the inclusion of area in the definition, the ability to detect smaller drought events more relevant for agricultural usage, and the ability to identify events and all pixels involved in the event at each time step—make this useful for the study of flash drought and particularly for the spatial distribution of its impacts.

3.2. Data Sets and Drought Indices

3.2.1. Calculation of the SSmI

The SSmI (AghaKouchak, 2014; Hao & AghaKouchak, 2013) is a drought index calculated using the same standardized method as the commonly used Standardized Precipitation Index (SPI) (McKee et al., 1993). The SSmI is based on the root zone soil moisture—defined by the data set authors and assumed in this study to be soil moisture from the top 100 cm of soil (Erlingis et al., 2021)—and exhibits high autocorrelation, indicating a heavy dependence on previous values (AghaKouchak, 2014). Mild drought is defined as an SSmI of 0 to -0.99 ; moderate drought is -1.00 to -1.49 ; severe drought is -1.50 to -1.99 ; and extreme drought is less than -2.00 .

The Standardized Drought Analysis Toolbox (Farahmand & AghaKouchak, 2015) is a generalized framework for calculating standardized drought indices. A main feature of this toolbox is that it eliminates the need for fitting distribution curves to the data, a challenge that can hinder the comparability of different standardized indices across variables (Bayissa et al., 2018; Farahmand & AghaKouchak, 2015; Hao & AghaKouchak, 2013; Stagge et al., 2015), by using the Gringorten empirical plotting position (Gringorten, 1963) rather than probability distribution curves to calculate the probability of occurrence. This study uses the modified SDAT method used in Ho et al. (2021) to calculate the SSmI from 1980 to 2012 on a 5-day, rather than 30-day, timescale. This modified method also includes the Weibull non-exceedance probability to deal with zero-data occurrences per Stagge et al. (2015) and uses a daily, rather than a monthly, time step to generate a daily time-step data set.

Components for calculating the root zone soil moisture were taken from the Western Land Data Assimilation System (WLDAS), a recently released fine-scale ($0.01^\circ \times 0.01^\circ$), daily land surface model based on remote sensing data developed for the study of near-surface hydrology. Meteorological forcing drives a land surface model containing leaf area index, vegetation class, and soil texture to simulate energy and water budget processes. As a collaborative effort between the National Aeronautics and Space Administration (NASA) and the California State Water Resources Control Board (SWRCB) (Erlingis et al., 2021), it is a special instance of NASA's Land Data Assimilation System (LDAS) that is customized for the Western United States for the purpose of sustainable groundwater planning in California (Erlingis et al., 2021). Root zone soil moisture was calculated as the sum of volumetric soil moisture in the top three layers of soil (total depth of 100 cm) and does not include additional input from irrigation.

3.2.2. Calculation of the NDVI Z-Score (zNDVI)

The NDVI is a measure of vegetation greenness from the combination of the red and near-infrared bands collected by satellite data, calculated as

$$\text{NDVI} = \frac{\rho_{\text{NIR}} - \rho_{\text{R}}}{\rho_{\text{NIR}} + \rho_{\text{R}}} \quad (7)$$

where the red bands indicate absorption by plant chlorophyll during photosynthesis and the near-infrared bands are affected by leaf structure. The NDVI ranges from 0 to 1, with 1 being the ideal value (Goldberg et al., 2010; Tucker, 1979). Key weaknesses of the NDVI include its sensitivity to soil brightness and color, atmospheric interference, and sensor calibration (Huang et al., 2020; Xue & Su, 2017). Despite the existence of other similar indices

that improve on these, the NDVI remains widely popular due to its ease of calculation and abundance of available data (AghaKouchak et al., 2015; Huang et al., 2020; Xue & Su, 2017). Studies using the NDVI and its derived products have indicated that even short dry spells can have damaging effects on crop health and production (Ji & Peters, 2003; Nicolai-Shaw et al., 2017; Orth & Destouni, 2018; Otkin et al., 2016; Vicente-Serrano et al., 2013), with some suggesting that certain vegetation types can attenuate drought effects (Pendergrass et al., 2020).

This study uses data from the Moderate Resolution Imaging Spectrometer (MODIS) (Spruce et al., 2016). It is a smoothed, gap-filled, composite data set composed of data from both the Terra and Aqua satellites. The satellites collected on an 8-day time step using a maximum value composite approach for the conterminous United States from 1 January 2000 through 31 December 2015 (Spruce et al., 2016), though for this study only values through 2012 were considered. Per year, there are 46 timesteps each representing 8 days (for the 46th timestep of the year, the first values of the next year are included). It was upscaled to the WLDAS grid using the weighted average method.

Because the NDVI value is a measurement for the period without historical context, further processing is needed to be able to compare it with drought indices (Huang et al., 2020; J. Peng et al., 2020; Peters et al., 2002). For this study, NDVI is prepared for comparison with drought indices by calculating the z -score of the observation in the style of Peters et al. (2002), where the z -score for a coordinate i for timestep j of 46 in year k can be calculated as

$$z\text{NDVI}_{ijk} = \frac{\text{NDVI}_{ijk} - \overline{\text{NDVI}}_{ij}}{\sigma_{ij}} \quad (8)$$

where $\overline{\text{NDVI}}_{ij}$ is the average NDVI for the given pixel at the given timestep across the entire observed period, and σ_{ij} is the standard deviation for the same pixel at the same timestep.

The z -score can be understood as the number of standard deviations an observed value is from the mean—in other words, the degree of abnormality. The z -score has been used for comparison of NDVI with other drought indices in several studies (Dong et al., 2019; J. Peng et al., 2020; Peters et al., 2002), though it should be noted that such comparisons are best limited to trend analysis due to the different calculation methods.

3.2.3. Division of Irrigated Agriculture Using the Global Food Security Analysis and Data

The Global Food Security Analysis and Data (GFSAD) 1 km crop extent data set (Teluguntla et al., 2015), masked to the study area, assigns irrigation status (watering method) to each pixel in the area. Major irrigation, minor irrigation, and rainfed pixels consist of more than 50% (by area) of cropland and are differentiated by how the cropland is irrigated (Teluguntla et al., 2015). Irrigation in this data set is explicitly defined as the “artificial application of any amount of water to overcome water stress” (Teluguntla et al., 2015), including land that is irrigated only once; rainfed areas are land that receives no additional water to overcome water stress. Major and minor irrigation differ not in the amount of water added, but rather the source of the water for irrigation (Teluguntla et al., 2015). Though the distinction between major and minor irrigation can be difficult to parse in many places, Teluguntla et al. (2015) explicitly name the CA Central Valley as a location where they are clearly distinguished. The decision to exclude minor irrigation, rather than lump it with major irrigation, is because minor irrigation sources are more likely to be privately owned and can be drawn with relatively fewer restrictions, making it more difficult to regulate. This study therefore only focuses on major irrigated—henceforth irrigated—agriculture (19% of study area) and rainfed agriculture (42.2% of study area).

3.2.4. Aridity

An aridity index (Le Houerou, 1996) was calculated to characterize the water-energy relationship of the study area (Figure 2), where aridity is the ratio of energy to available water:

$$\text{Aridity} = \frac{\sum \text{Precipitation}}{\sum \text{Potential ET}} \quad (9)$$

A smaller aridity index indicates that there is more energy than water and therefore more arid; a larger aridity index indicates more water and therefore more humid. Potential ET was calculated using the FAO-56 Penman–Monteith method (Zotarelli et al., 2010) with components from WLDAS and the SRTM Digital Elevation Model (NASA-JPL, 2013). More than half of the region (55.92%) is classified as semiarid (aridity of 0.2–0.5), less than half (31.32%) is classified as arid (aridity of 0–0.2), 10.55% is considered dry sub-humid (aridity of 0.5–0.6),

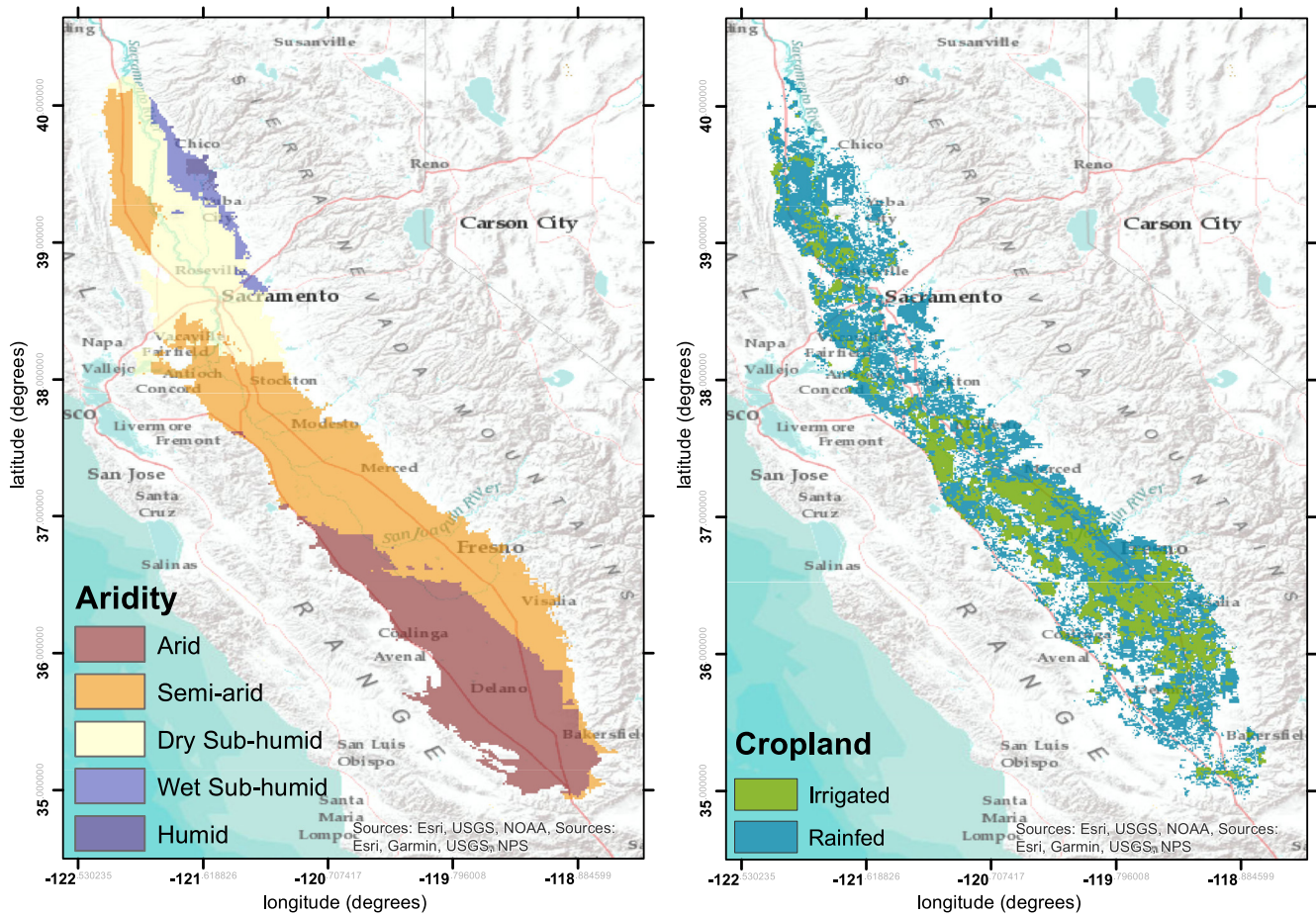


Figure 2. The aridity index (ratio of total precipitation to total potential evapotranspiration) and cropland classifications for the study area.

1.43% is wet sub-humid (aridity of 0.6–0.75), and the rest (0.78%) is humid (aridity >0.75). The irrigated regions are primarily in arid (29.08% of all irrigated area), semiarid (68.86%), and dry sub-humid (1.98%) climates, with only a few pixels in more humid climates. Rainfed areas are also mainly concentrated in the arid (25.57% of all rainfed area), semiarid (63.30%), and dry sub-humid regions (9.86%), but also exist in wet sub-humid (0.98%) and humid regions (0.29%).

3.3. Drought Characteristics

Droughts in this study are further studied using three degrees of dimensionality: by drought type (flash or normal drought); by drought severity class (moderate, severe, extreme, or a combination of all severities above the threshold dryness described in Section 3.2.1); and by irrigation method as defined by the GFSAD data set (major irrigation and rainfed) (Teluguntla et al., 2015).

The analysis of drought events requires the refining of the data sets to relevant events. For each drought event identified using the drought identification method described in Section 3.1, an event time series is generated via a collection of the SSMI time series for every pixel in the event for the entire drought duration, regardless of how long the pixel is involved. This process is repeated for all drought events to ensure that analyses are conducted for drought events only.

3.3.1. Average Relative Drought Duration

Drought events, particularly normal droughts as defined in the method described in Section 3.1, can vary greatly in duration. Moreover, the flexible spatial and temporal definitions of the method allow situations where a pixel may only spend one or two time steps in a drought event. This makes it difficult to compare the effects of duration

between different events, particularly between flash and normal droughts. Here, we propose an average relative drought duration (ARDD) as a metric to generalize duration over multiple events for investigating the corollary to H1.

The relative drought duration (RDD) is a characteristic that expresses how long a pixel is involved in a drought event relative to the total drought duration. It can be considered a measure of a pixel's persistence or prominence in a drought event. The relative duration for a pixel i in a single drought event is calculated as the fraction

$$RDD_i = \frac{t_i}{t} \quad (10)$$

where t_i is the total number of time steps spent in drought and t is the total duration of the drought event. The ARDD is then calculated across all drought events n in which the pixel exists:

$$ARDD_i = \frac{\sum_1^n RDD_i}{n} \quad (11)$$

If a positive relationship between ARDD and vegetation response can be established (corollary to H1), a higher ARDD can indicate that a pixel is more likely to suffer from long-term drought effects.

3.3.2. Correlation to zNDVI

Calculation of the Pearson correlation coefficient r is commonly used to determine the strength of relationship between two variables, with 1.0 being the highest possible correlation, -1.0 being the highest possible anticorrelation, and 0 indicating no relation (Taylor, 1990). Such information is useful for determining the effects of drought on vegetation health: because the correlations are calculated exclusively during drought events (i.e., when SSmI values are negative), a positive correlation during a drought event would indicate a deterioration of vegetation health, while a negative correlation would indicate improved conditions despite drought conditions. Only statistically significant ($p < 0.05$) correlations between zNDVI and the SSmI (calculated during all drought events between 1 January 2000 and 31 December 2012) were considered. This zNDVI-SSmI correlation will be the key metric in investigating drought impacts on vegetation (H1, H2, and H3).

An additional 8-day time series for the SSmI to match the 8-day resolution of the zNDVI data set was generated by selecting every eighth value to correspond with the zNDVI. Because the SSmI in this study includes the effect of the previous 4 days (for a visual representation of this, please refer to Figure 3 in Ho et al. (2021)), taking the median or average of the 8 days would result in soil moisture data outside of the 8-day resolution being considered by the NDVI. Thus, each year has 46 values for SSmI, and zNDVI, with the 46th value extending into the beginning of the next year.

4. Results and Discussion

4.1. Identified Drought Events

Of the 41 drought events, only 7 were flash droughts (Table 1). Bolded events indicate events with a sufficient intensification rate, but were too long to be considered flash droughts under the current methodology. Flash droughts occur at an average frequency of once every 5 years, which is in agreement with X. Xiao et al. (2019). Comparison with the United States Drought Monitor (Svoboda et al., 2002) show that the method is generally in agreement with rapid increases in USDM-categorized area (for more, see Figure S3 in Supporting Information S1), and the beginning of the 2011–2017 drought (events 38–41) is adequately captured by the method, both indicating that the method is acceptable for identifying both normal and flash droughts.

Eight normal droughts existed that satisfied the AIIR condition but not the maximum duration condition, that is, these droughts were too long to become classified as a flash drought. Three of these events are within 10 days above the 60-day maximum, which is a proposed limit in this method that has—thus far—no strong theoretical basis. For example, three rapidly intensifying drought events were identified in the 1990s, but were too long to be considered flash droughts due to the duration period in the method. Under a more lenient duration criterion, they could thus be considered flash drought. We can also be sure that events with a short development duration are not flash drought events due to the intensification criteria: because these criteria are calculated over the development stage, the definition of flash drought remains limited to events whose development periods are both brief and

Table 1
All Flash and Normal Drought Events Found by the Method, Along With the Duration of Their Development Phase and Maximum Area

ID	Start date	End date	Type	Duration (days)	Development Phase (days)	Maximum area (% total)
1	5/23/1980	1/31/1981	Normal	254	242	96.9
2	6/7/1981	7/8/1981	Normal	32	9	7.4
3	6/4/1982	7/1/1982	Flash	28	21	16.2
4	7/18/1982	9/18/1982	Normal	63	61	26.6
5	2/23/1985	3/19/1985	Flash	25	13	61.7
6	6/5/1985	7/23/1985	Normal	49	18	23.2
7	7/30/1986	9/10/1986	Flash	43	1	4.6
8	10/29/1986	1/5/1987	Normal	69	22	90.7
9	4/20/1987	6/25/1987	Normal	67	13	67.0
10	2/12/1988	4/20/1988	Normal	69	54	89.1
11	1/30/1989	3/6/1989	Normal	36	33	33.2
12	4/16/1989	7/5/1989	Normal	81	10	54.5
13	12/5/1989	1/13/1990	Normal	40	27	27.9
14	12/15/1990	3/4/1991	Normal	80	73	99.9
15	4/18/1992	6/28/1992	Normal	72	51	73.7
16	5/9/1993	6/5/1993	Normal	28	17	17.9
17	6/15/1993	10/16/1993	Normal	124	114	56.0
18	6/1/1994	10/4/1994	Normal	126	32	14.7
19	5/30/1995	12/17/1995	Normal	202	192	95.5
20	6/20/1998	11/11/1998	Normal	145	127	82.5
21	12/15/1998	4/8/1999	Normal	115	30	69.4
22	4/18/1999	5/29/1999	Normal	42	13	7.8
23	10/10/1999	11/8/1999	Normal	30	19	11.1
24	11/25/1999	1/26/2000	Normal	63	49	91.1
25	4/2/2000	5/19/2000	Normal	48	5	97.7
26	12/17/2000	1/12/2001	Flash	27	24	90.0
27	5/25/2003	6/22/2003	Normal	29	6	4.2
28	10/10/2003	11/4/2003	Flash	26	22	57.7
29	3/12/2004	7/15/2004	Normal	126	15	54.8
30	5/24/2005	12/31/2005	Normal	222	209	79.2
31	1/26/2006	3/6/2006	Flash	40	24	49.7
32	9/7/2006	10/7/2006	Flash	31	28	10.1
33	11/5/2006	12/14/2006	Normal	40	36	77.0
34	1/12/2007	4/23/2007	Normal	102	69	99.6
35	5/1/2007	6/26/2007	Normal	57	27	10.2
36	3/13/2008	5/25/2008	Normal	74	42	65.1
37	1/16/2009	2/15/2009	Normal	31	8	44.6
38	6/22/2011	10/6/2011	Normal	107	98	46.4
39	10/19/2011	11/12/2011	Normal	25	17	12.1
40	12/1/2011	3/20/2012	Normal	111	91	99.8
41	11/8/2012	12/15/2012	Normal	38	23	7.3

Note. Bolded events are events that fit the intensification criteria for flash drought, but exceeded the maximum duration criteria.

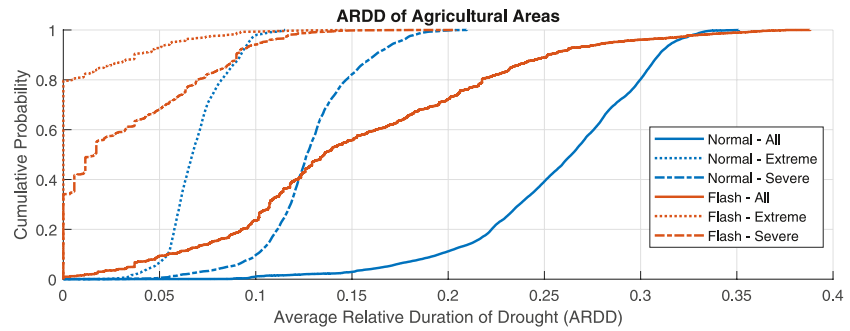


Figure 3. Cumulative distribution functions for relative drought duration of pixels under normal and flash drought. Additional lines indicate the average relative drought duration (ARDD) of severe (dotted) and extreme (dashed) conditions during the respective drought events.

intense. Other events, particularly the longer ones, may be normal drought events with a sudden intensification period within them, as mentioned by Otkin et al. (2018); however, the method used in this paper is currently unable to properly classify such events. For the purposes of this study, the bolded events will be considered normal events.

In general, the duration of observed droughts ranges from the minimum length for a drought event (25 days) to 254 days, while droughts occur up to more than once per year. Though the spatial extent of droughts varies greatly, soil moisture flash droughts occupy an average of 41% of the study area compared to 51% of all droughts and 53.9% of normal droughts. Both types of drought feature relatively similar temporal spans of their development stage (65% flash and 59% normal). Drought events that can be analyzed with zNDVI data (2000–2012) have relatively short recovery periods, indicating that such results will be valid primarily for drought onset and unable to account for potential lagged effects of vegetation such as those found by C. Peng et al. (2014). Proper accounting for such effects also requires detailed field-scale knowledge of crop rotations and crop-unique parameters such as vapor pressure deficit and stomatal conductance (J. Zhang et al., 2021), which lies outside of the scope of this paper. However, understanding the short-term and onset effects of flash droughts can help identify early flash drought and thus signal to water managers and farmers that rapid action may be necessary.

4.2. Average Relative Drought Duration

Cumulative distribution functions of time a pixel spent in drought (ARDD) are plotted for all pixels in both drought types (Figure 3). Additional categorical divisions are made for severe and extreme drought conditions (i.e., ARDD calculated for $SSmI \leq -1.5$ and $SSmI \leq -2.0$, respectively). The shape of the curves indicates that pixels in normal drought not only spend relatively more time in drought conditions but are also less statistically variable (H1).

For normal drought events, relative duration information should be viewed with caution, as these cover a broad range of durations from 25 to over 200 days in length. Pixels spend 10%–35% of the total duration in drought. Using this relative duration statistic for the median event (69 days), this would mean anywhere from 7 to 25 days in drought. The relative briefness in drought events, especially those in extreme and severe intensity, implies that the event has a quick and intense onset; this should not be surprising, considering that is the type of drought events that the identification method was designed to find.

Flash drought events show a drastically different behavior. These pixels spend up to 40% of their time in drought events. Assuming the median duration of 28 days, this means they will spend anywhere from 1 to 12 days in a drought event, with a relatively even probability distribution inferred from the curves' linearity. This is astoundingly short compared to the traditional drought events. However, our interest in this study for large-scale spatial patterns makes data from even a pixel with a single day in drought valuable: similar to how questions of fluid dynamics can be viewed through either an Eulerian or Lagrangian point of view, we posit that droughts can be viewed either from the point of view of a singular point (pixel) or as a moving mass. ARDD here serves to describe the behavior of the moving mass at a particular point.

Roughly 35% of pixels never reach severe drought conditions (this number increases to 80% for extreme conditions), indicating that these have a quick onset rather than a rapid intensification of drought. This is possible due

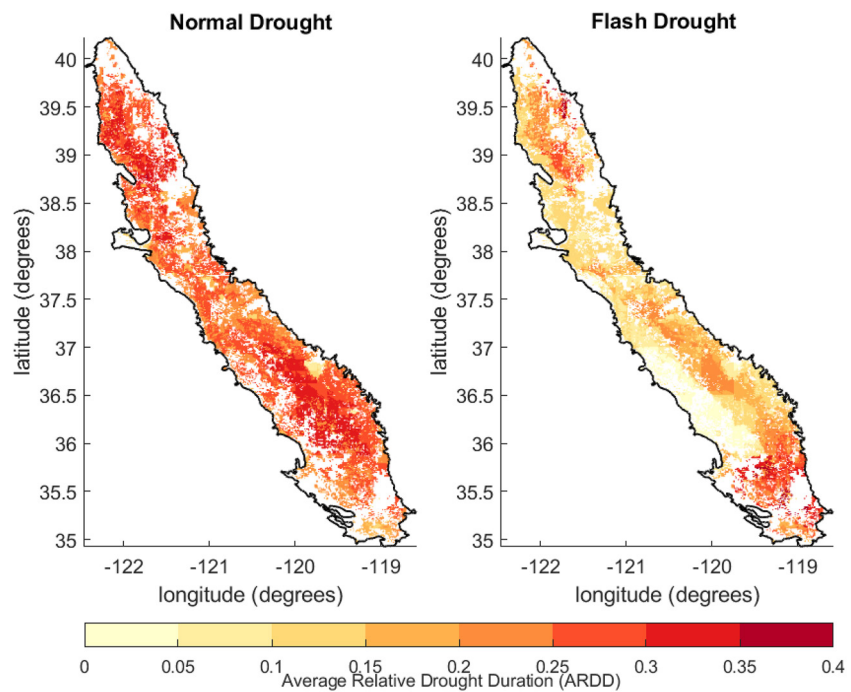


Figure 4. Spatial distribution of average relative SSMI-defined drought duration, differentiated by normal drought (left) and flash drought (right) for irrigated and rainfed pixels.

to the definition of DPI in the identification method allowing an increase of intensity to occur either by adding a pixel or by increasing the pixel's SI value. Because there is no specific weighting method, the effect of adding a new pixel experiencing drought will always be at least -1 , whereas the effect of decreasing the SI of an existing pixel will generally be less (e.g., decreasing SI from -1.2 to -1.5 would only decrease the DPI value by -0.3). This may prove problematic for certain applications of the method, but due to our assumption that water managers care equally about both large, moderately affected areas and small, severely affected areas, this does not significantly impact our analyses.

4.2.1. Spatial Distribution of ARDD

Spatial maps of the ARDD for both normal and flash drought are shown in Figure 4. Flash drought shows significant spatial variability. Pixels experience relatively longer drought duration in the southern and northern tips, which are the climatic extremes (driest in the south and most humid in the north), and along the inland center. Shorter durations are distributed relatively evenly throughout the rest of the catchment, though the southwestern edge of the catchment (the most arid) seems to experience significantly shorter durations. The spatial patterns seem to correspond less to those of aridity (Figure 2) and more to the PWP (Figure 1). (For more details, please see Figure S4 in Supporting Information S1.) This makes sense, given that the events were defined by soil moisture anomalies and that different soil characteristics (roughly represented by the wilting point) have different water retention capacities. Different soils will therefore be more sensitive to shorter time scales. However, such patterns cannot be identified in normal, longer drought. This suggests, in support of H1, that the additional length of normal drought allows the ARDD to become independent of soil type and thus more spatially homogeneous.

4.3. Correlation to zNDVI

Spatial maps of the zNDVI-SSmI correlation during flash and traditional drought are shown in Figure 5.

Overall, normal drought correlations are both more negative and less spatially variable than flash drought, which agrees with H1. The correlation results in normal drought show slightly more positive correlations for rainfed pixels over irrigated pixels (for more, see Figure S5 in Supporting Information S1), suggesting a potential dampening effect of irrigation (H3). This roughly corroborates the findings of Lu et al. (2020); rainfed crops are more affected by drought than irrigated crops. A possible explanation could be that areas with rainfed irrigation are

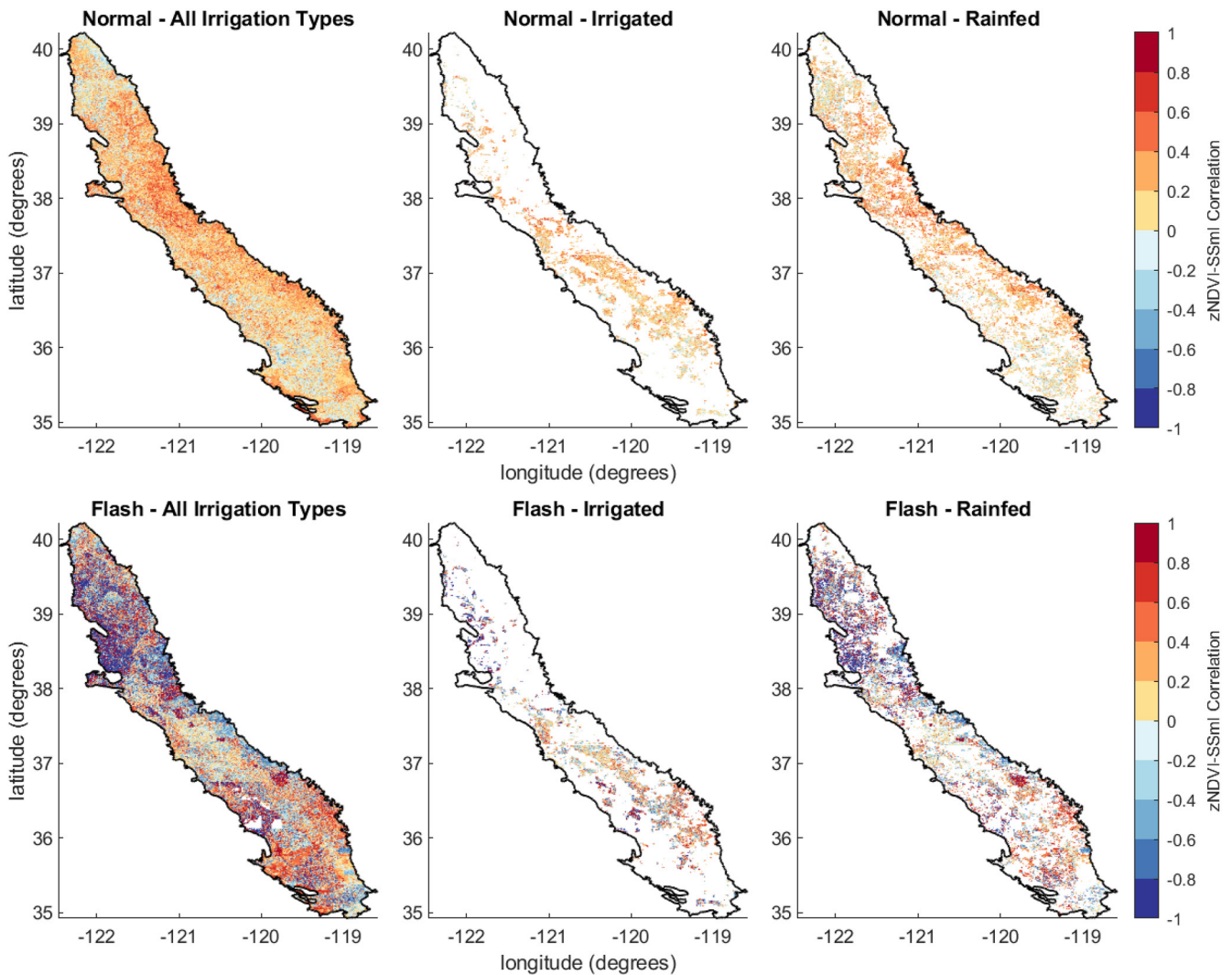


Figure 5. Significant correlations of SSMI and zNDVI ($p < 0.05$) during normal and flash drought events and for different irrigation types.

in more humid areas with less need for additional irrigation (H2); however, the lack of additional water during drought may mean crop growth will be limited by water availability. The range of correlation coefficients may also be a result of different crop types and timing: previous work has indicated that different crops respond faster to soil moisture conditions (C. Peng et al., 2014), and that crops exhibit higher sensitivity to moisture conditions in their reproductive stages, which are highly seasonal (Ji & Peters, 2003). This analysis was unable to include details on specific crops due to limitations on available crop data during each drought event.

Correlation with SSMI during flash drought shows very strong anticorrelation in the north, weaker correlations and anticorrelations in the center, and a stronger tendency toward positive correlations in the south. These spatial patterns are partly mirrored by patterns of aridity (Figure 2), lending credence to H2. Rainfed pixels again show stronger correlation—both negative and positive—to zNDVI than irrigated pixels (H3). Correlations for flash drought show visible differences between irrigation types, which shows that rainfed cropland tends to be anticorrelated.

Such results are also consistent with previous work on the relationships between drought and agriculture. Dong et al. (2019), for example, found that during the landmark 2012–2016 California drought, severe NDVI decreases accompanied by drying in the southern end of the state while the northern end saw increased NDVI. They posited that the counterintuitive improvement of vegetative health in the north, despite water shortages, could be a result of warmer temperatures assisting plant growth. While the timescales of drought are vastly different, such findings

are consistent with the strong anticorrelation with SSmI in the northern end—indicating an increase in NDVI despite a decrease in SSmI—and the tendency toward positive correlation in the southern end. An additional study suggests that this may also be related to the aridity of the region (Orth et al., 2020): the northern region, which is less arid, suffers significantly less from drought and can even benefit from relatively drier conditions, depending on the situation. These explanations, along with the assumption that flash droughts can be temperature driven (Mo & Lettenmaier, 2015), can help explain why there are such clear differences in regions. However, without investigation of the actual water supply (in this case soil moisture), a causal relationship between flash drought and zNDVI cannot be established due to the potential misrepresentation of actual water stress inherent in standardized indices (Zang et al., 2019). This will be explored in Section 4.3.1. Low SSmI values in the humid north may still indicate sufficient plant available water, but may be associated with warmer temperatures and more photosynthetically active radiation (Ford & Labosier, 2017). Thus, relatively drier conditions could—under certain situations—stimulate plant growth.

A weakness of these correlation results is that these time series do not have many data points. Each drought event lasts a minimum of 25 days, with flash droughts capping at 60 days. Given that the NDVI data set only collects values once every 8 days, and values are only extracted from within the drought event, a flash drought event will only have at minimum 3 and at maximum 7 data points. Because flash drought events are few, the number of data points for correlation is also few—this could mean that the correlations could change significantly as more events are identified either over a larger spatial domain or with longer future records.

Previous literature has suggested that there is a significant lag between water shortages and effects on NDVI that vary with vegetation species (Ji & Peters, 2003; C. Peng et al., 2014). The inclusion of the recovery phase in the drought identification method allows at least partial inclusion of any potential lag times in vegetation response in this study. Thus, it can be said that the correlations in this study focus more on the immediate onset and short-term effects of flash drought. Further exploration of the medium-to-long-term impact of flash drought (i.e., the lagged vegetation impacts) could be considered in future studies by adding more time steps before and/or after the duration of the drought event to include potential lagging effects, and by extending the observed time period to include more flash drought events.

4.3.1. Soil Moisture Conditions

Maps describing the average volumetric soil moisture content for irrigated and rainfed cropland during the entire observation period, during exclusively flash drought events, and the difference between the two can be seen in Figure 6. It should be noted that only flash droughts from the NDVI observation period (2000–2012) are used here, as this investigation is intended to explore the correlation results (H2) in further detail.

In general, the high-anticorrelation regions in the northern section do experience a significant drop in soil moisture content under flash drought; however, the remaining soil moisture content during flash drought still generally remains close to or above 20%. While these areas do have the highest decreases in soil moisture, the remaining soil moisture is generally above the estimated PWP (Figure 1). This suggests that the average water deficit during the flash droughts in this northern region is, despite the SI value, not severe enough to cause permanent damage to the crops cultivated. In other words, dry soil moisture conditions (particularly if there is still plant available water) do not inherently result in plant stress, which is in agreement with H2 and with Zang et al. (2019), and may also depend on soil texture.

Interestingly, an increase in average soil moisture is seen in the central region of the study area during flash drought events—while it may seem counterintuitive, this may be attributed to the lack of seasonal context that an arithmetic mean has in comparison to the standardization process used when calculating SSmI. In other words, the soil moisture conditions during flash drought was dry for that particular day of the year, but overall higher than the arithmetic average for the total observation period (e.g., a soil moisture content of $0.3 \text{ m}^3/\text{m}^{-3}$ in a historically wet month, e.g., January, could result in $\text{SSmI} = -1.5$, but the average soil moisture content over 32 years could be $0.2 \text{ m}^3/\text{m}^{-3}$). While this is indeed a robust feature of the standardization process, it does call for careful interpretation, as drought conditions in an SI may not always indicate in-situ dryness (Zang et al., 2019).

4.3.2. Relationship to ARDD

Density plots demonstrating the relationship between zNDVI-SSmI correlation with ARDD (Figure 7) sought to answer H1. Normal drought (a and c) showed a generally decreasing average correlation with increasing relative

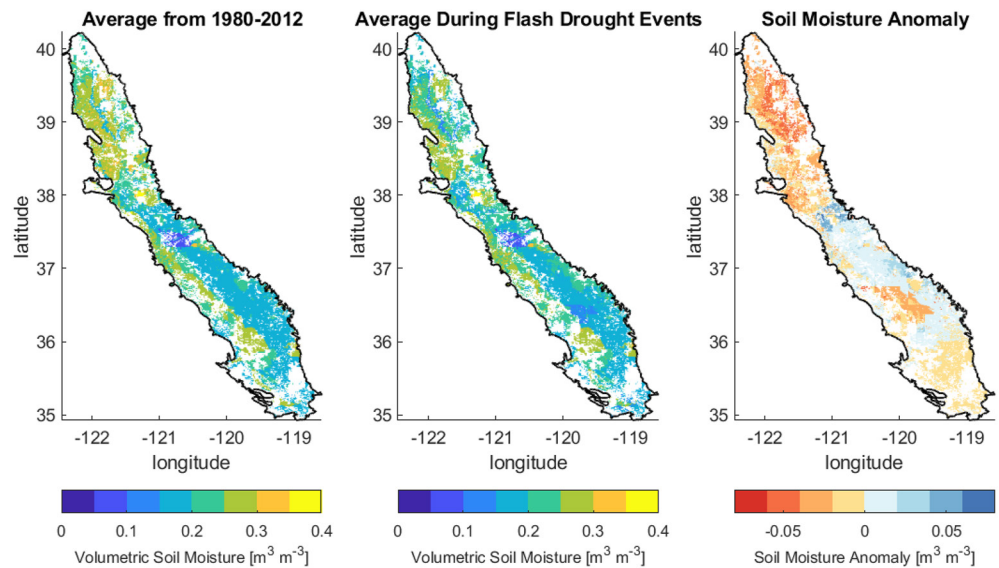


Figure 6. Maps displaying average volumetric soil moisture content [m^3/m^{-3}] for the entire observation period (1980–2012), for exclusively flash drought durations during the NDVI observation period (2000–2012), and the anomaly (difference from the long-term average). Red indicates regions where average soil moisture during flash droughts is drier than the long-term average; blue indicates wetter. Only irrigated and rainfed cropland is shown.

duration; however, the correlation remained overall positive and rather densely compacted. This decrease is contradictory to the expectation (corollary to H1): instead of worsening impacts with increased relative duration, pixels spending longer in drought seem to exhibit a weaker correlation. A potential explanation could be that the longer overall drought durations erode the relationship between SSMI and NDVI. Moderate drought conditions, sustained over weeks, can cause deterioration in crops; if this has already occurred, an increase in dryness would likely not cause further deterioration. Flash drought, on the other hand, shows correlations that are more frequently negative or close to zero, with considerable noise outside of a few small hotspots (b and d). This noise could be due to the lag in response time between soil moisture and vegetation condition (Otkin et al., 2016; C. Peng et al., 2014); however, because the flash drought detection method accounts for a recovery period, this may already be partially considered. Particularly interesting is the increased noise in irrigated flash drought (b) over irrigated normal drought (a)—we hypothesize that this is the result of the variety of irrigation techniques and crop types decoupling responses to drought by reducing the deficit to varying degrees. Overall, while normal drought did indeed show more negative consequences to vegetation than flash drought, longer relative duration within drought types did not necessarily mean a more detrimental result to vegetation (H1).

4.4. Relationships of Characteristics to Aridity

Drought characteristics were analyzed with respect to aridity to further contextualize the differences between flash and normal drought on agriculture, whether rainfed or irrigated. The aridity is an expression of average available energy and water over a longer time period—previous studies have indicated a relationship between aridity and vegetation response, with more arid regions typically exhibiting a quicker and stronger response of vegetation to dry conditions (O & Park, 2023; Orth et al., 2020; Vicente-Serrano et al., 2013). Many of the characteristics have shown statistical differences between drought types and vegetation responses; however, the variable spatial distribution of these characteristics implies a spatial reason for these differences. Because this variation seems to be aligned with the spatial distribution of aridity in the study region, the further investigation of characteristics of aridity in this section can help illustrate whether these statistical differences are due to geographic location and climate (which in this study area is related to aridity) or irrigation.

4.4.1. Aridity and Relative Duration

ARDD in normal drought remains relatively stable throughout different aridity conditions and exhibits similar patterns in both irrigation types (Figure 8). Because the data set does not include the effects of irrigation on soil

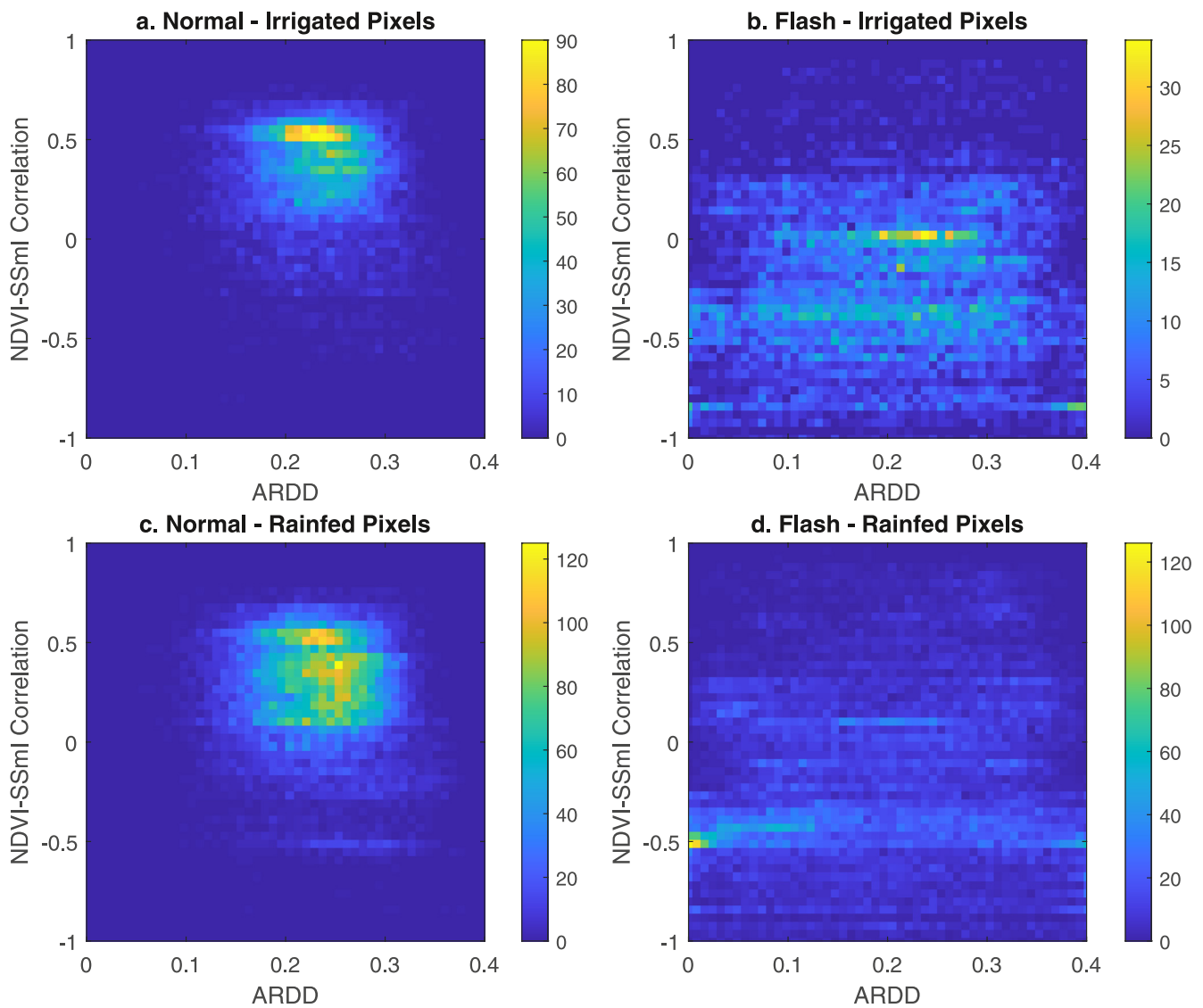


Figure 7. Density map illustrating the relationships between zNDVI-SSmI correlation and relative duration for both drought types (normal, a and c; flash, b and d) and over different irrigation types (irrigated, a and b; rainfed, c and d). Note the different color axes.

moisture, this similar behavior is rather expected. The longest relative durations for flash drought are associated with the highest aridity index (most humid conditions), where increased duration implies increased humidity. This behavior seems to be in contrast with Orth et al. (2020), who found an increase in relative duration with increasing dryness. While in Figure 8, there is a slight increase in relative duration with increasing dryness (average ARDD increasing from 12% at aridity index 0.20%–20% at aridity index 0.15) in flash drought, this trend is not nearly as strong as that of increasing wetness (higher average ARDD at higher aridity index ranges). This seemingly strong relationship between relative duration and humidity may be due to the average soil moisture anomaly in each region—due to the larger deficit in humid regions; it may take longer for the volumetric soil moisture to return to normal conditions. However, the relatively small sample sizes in dry sub-humid, wet sub-humid, and humid regions indicate that such statements are merely tentative, and that further study should be conducted in wetter climates for more conclusive findings. For now, it can be hypothesized that the relative duration is more strongly related to soil type than to aridity, as there seems to be no strong relation in more humid regions.

4.4.2. Aridity and Correlation to zNDVI

Normal drought for all irrigation types maintains a slightly positive median correlation between SSmI and vegetation greenness across all aridity categories (Figure 8), with slight swelling in the semiarid region (~0.35) and

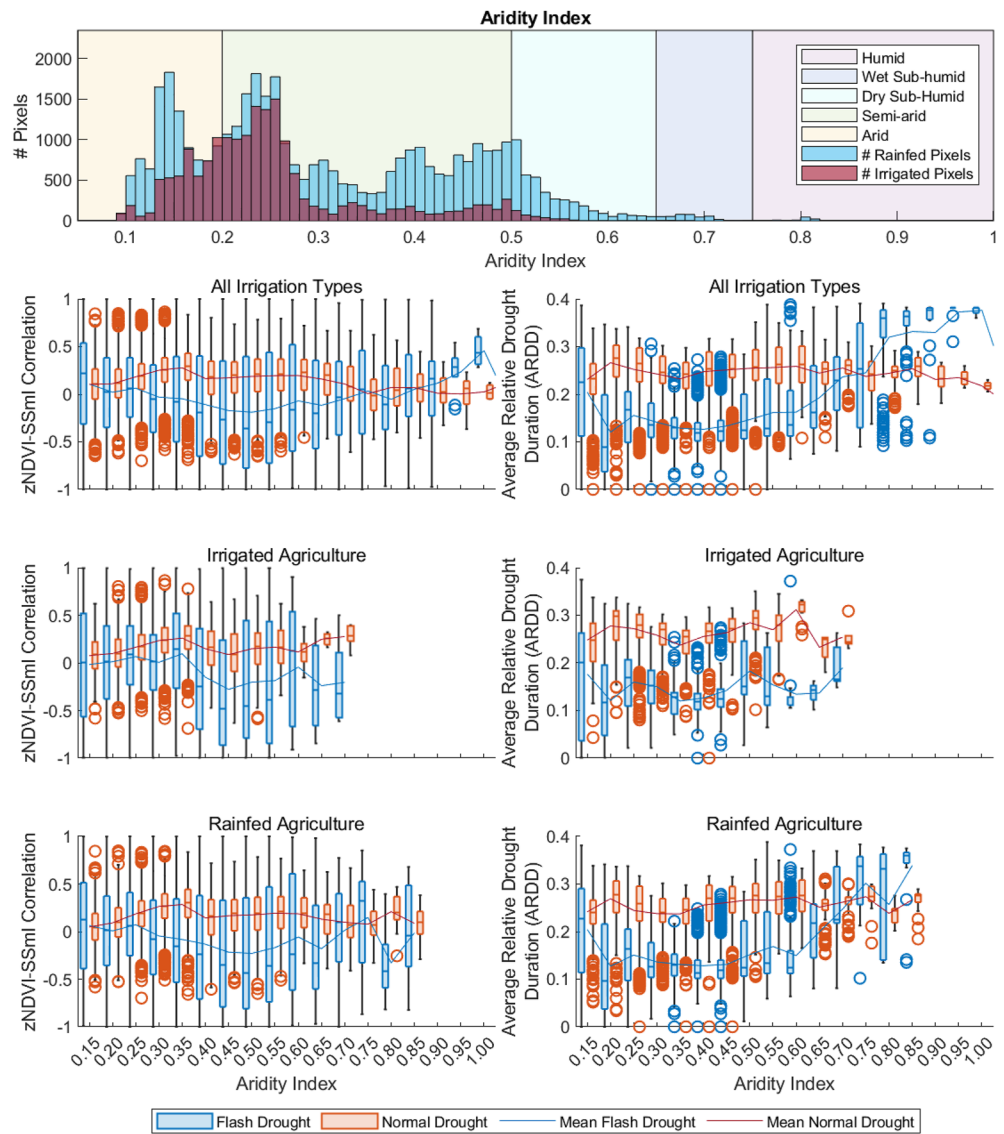


Figure 8. Relationships of average relative drought duration (ARDD) and zNDVI-SSmI correlation to aridity.

slight decreases in the wetter semiarid and dry sub-humid regions demonstrating the impact of aridity (H2). Overall, the irrigated regions have a weaker correlation, indicating that the added water does indeed temper the potential adverse responses (H3). However, the relatively high correlations for the most humid regions in irrigated areas indicate that the irrigation there may not be able to compensate for the sustained deficits. This could potentially result from more water-intensive crops being grown in this region that require more water than normal.

The low correlations for normal drought in the most arid regions seem to contradict Orth et al. (2020)'s and Vicente-Serrano et al. (2013)'s findings that arid regions have quicker and stronger responses to drought conditions (for both crops and forests). However, this could be due to the fact that these studies focus on drought on longer time scales (months vs. sub-monthly in this study) and on larger regions (global studies vs. this regional study). The shorter accumulation periods used for SSmI and the drought detection method being optimized for flash drought may result in events that are too sensitive to short-term changes in soil moisture and subsequently not result in the higher deficits found in longer accumulation periods. It may also be due to the diminishing difference in actual soil moisture indicated by a standardized value: as soil moisture decreases, the difference in soil moisture required to render more intense drought also decreases. Thus, actual soil moisture deficits in arid regions may actually be quite small (Figure 6) and the vegetation grown there may be much more suited to adapt to the already-dry conditions (H2).

Flash drought for all irrigation types shows slightly positive correlations in the arid and driest semiarid regions that become increasingly negative in the semiarid and dry sub-humid regions and increase drastically in the humid regions (H2). That the most positive correlations are in the most arid and most humid regions agrees with Vicente-Serrano et al. (2013)'s findings that these regions are most sensitive to drought conditions. Our results are also consistent with O and Park (2023)'s findings that the flash drought onset—on which our study focuses—is strongly associated with increased vegetation condition in locations where soil moisture is sufficient for plant growth. Overall, irrigated agriculture seems to be more positively affected by flash drought, indicated by the steeper decrease in correlation between the drier and the wetter semiarid regions than in rainfed agriculture. This seems to give credence to Dong et al. (2019)'s hypothesis that this is a result of wetter regions having more available sunlight and energy for photosynthesis, resulting in improved vegetation condition, since irrigation bridges the water-energy gap and thus allows a speedier recovery from drought conditions. However, when the environment becomes dry enough (aridity <0.35), irrigation loses its effectiveness on the vegetation condition (H3), resulting in more positive correlations (for an alternate visualization, see Figure S6 in Supporting Information S1).

5. Conclusions

This study has provided the following insights into the hypotheses outlined in the introduction:

- H1—The results indicate that normal drought does indeed have more spatially homogeneous drought characteristics (both ARDD and vegetation response expressed as the correlation between zNDVI and SSmI) and a more negative impact on vegetation than flash drought. However, our results are not consistent with the corollary—that regions with a higher relative duration within a drought type (flash or normal) will experience stronger (more adverse) responses to vegetation, expressed as the zNDVI-SSmI correlation. According to our density plots, effects to vegetation seem to temper with increasing relative duration in normal drought (potentially due to length of stress decoupling the response), while there is little observable trend in flash drought aside from a strong beneficial response at the highest relative duration.
- H2—Signals of vegetation responses to increasing SSmI dryness show considerable variation with aridity. As hypothesized, agriculture in humid regions does benefit from flash drought events due to a lack of a true plant water deficit, which is dependent on soil texture, and a short relative duration. Vegetation responses in hyper-arid sections experiencing normal drought also seem to show a more muted response than expected—this may also be related to the actual deficit in soil moisture being quite small. However, due to this study's focus on the immediate effects of drought, these analyses lack the potential effects of lagged vegetation responses.
- H3—Irrigation does indeed seem to temper adverse vegetation responses to both types of drought; however, the impacts seem to differ depending on the aridity. Overall, irrigation does reduce adverse vegetation response in normal drought aside from the exception of wet sub-humid regions (which may simply be too sparsely populated to form a representative sample). In flash drought, irrigated agriculture performs better than rainfed in most aridity regimes; however, once the climate reaches a certain dryness, irrigation seems to be less impactful.

This study is primarily limited by the available data: while the WLDAS data set is the highest-resolution and longest-running available in the region, it is still a reanalysis data set and, despite high performance in ET and leaf-area-index measures, does not currently directly include soil moisture observations or contributions from irrigation. This could affect drought identification and relative duration information for irrigated areas. Moreover, the small number of flash drought events analyzed in this study could have produced less robust results.

However, the elucidation of the potential effects of flash drought in comparison to normal drought provided by this study may prove useful insights into the impacts of flash drought, particularly for agricultural regions. The analysis of vegetation condition in different aridity regions during flash drought provides potentially generalizable insight into how the local climate can impact vegetation responses to drought. The changing effect of irrigation on vegetation during drought based on a location's aridity shows that, while it certainly can overcome negative effects in some regions, it may not be as impactful as expected in others. This study has shown that this could be due to the inability of standardized definitions to communicate or show deficits that will actually hamper vegetation growth. Investigations of drought on vegetation should therefore not limit their analyses to PWP and standardized indices, but also consider the actual available soil moisture and soil texture when drawing conclusions. Such investigation, in the face of the distinctly different characteristics of flash and traditional drought, may prove useful for preparing adaptation strategies in the future.

Conflict of Interest

The authors declare no conflicts of interest relevant to this study.

Data Availability Statement

Soil moisture data and components to calculate potential ET (for aridity calculation) from WLDAS used for drought identification and analysis in the study are available at NCCS Dataportal (https://portal.nccs.nasa.gov/datashare/WLDAS/wldas_domain/). The DEM—also used for potential ET calculation—is available through the USGS EarthExplorer (<https://earthexplorer.usgs.gov/>; Data Sets > Digital Elevation > SRTM > SRTM 1 Arc-Second Global). The crop mask used to identify irrigated and rainfed cropland (GFSAD1KCM) is available through the LP DAAC (<https://lpdaac.usgs.gov/products/gfsad1kcmv001/>). Smoothed and gap-filled MODIS NDVI data used for vegetation condition are available through ORNL DAAC (<https://doi.org/10.3334/ORN LDAAC/1299>). Soil texture data is available through the California Soil Resource Lab (<https://casoilresource.lawr.ucdavis.edu/soil-properties/>). A collection of scripts used to generate the data produced in this study can be found online (<https://github.com/sarahquynhngiang/FlashDroughtCA/tree/726d58d23bc5b9113f0ee54cc8db06b50558e313/Scripts>).

References

- AghaKouchak, A. (2014). A baseline probabilistic drought forecasting framework using standardized soil moisture index: Application to the 2012 United States drought. *Hydrology and Earth System Sciences*, 18(7), 2485–2492. <https://doi.org/10.5194/hess-18-2485-2014>
- AghaKouchak, A., Farahmand, A., Melton, F. S., Teixeira, J., Anderson, M. C., Wardlow, B. D., & Hain, C. R. (2015). Remote sensing of drought: Progress, challenges and opportunities. *Reviews of Geophysics*, 53(2), 452–480. <https://doi.org/10.1002/2014rg000456>
- Bayissa, Y., Maskey, S., Tadesse, T., van Andel, S., Moges, S., van Griensven, A., & Solomatine, D. (2018). Comparison of the performance of six drought indices in characterizing historical drought for the Upper Blue Nile Basin, Ethiopia. *Geosciences*, 8(3), 81. <https://doi.org/10.3390/geosciences8030081>
- Buras, A., Rammig, A., & Zang, C. S. (2020). Quantifying impacts of the 2018 drought on European ecosystems in comparison to 2003. *Biogeosciences*, 17(6), 1655–1672. <https://doi.org/10.5194/bg-17-1655-2020>
- Chen, L. G., Gottschalck, J., Hartman, A., Miskus, D., Tinker, R., & Artusa, A. (2019). Flash drought characteristics based on U.S. Drought monitor. *Atmosphere*, 10(9), 498. <https://doi.org/10.3390/atmos10090498>
- Christian, J. I., Basara, J. B., Otkin, J. A., & Hunt, E. D. (2019). Regional characteristics of flash droughts across the United States. *Environmental Research Communications*, 1(12), 125004. <https://doi.org/10.1088/2515-7620/ab50ca>
- Cody, B. A., Folger, P., & Brougher, C. M. (2015). *California drought: Hydrological and regulatory water supply issues*. Congressional Research Service.
- Dong, C., MacDonald, G. M., Willis, K., Gillespie, T. W., Okin, G. S., & Williams, A. P. (2019). Vegetation responses to 2012–2016 drought in Northern and Southern California. *Geophysical Research Letters*, 46(7), 3810–3821. <https://doi.org/10.1029/2019gl082137>
- Erlingis, J. M., Rodell, M., Peters-Lidard, C. D., Li, B., Kumar, S. V., Famiglietti, J. S., et al. (2021). A high-resolution land data assimilation system optimized for the western United States. *Journal of the American Water Resources Association*, 57(5), 692–710.
- Farahmand, A., & AghaKouchak, A. (2015). A generalized framework for deriving nonparametric standardized drought indicators. *Advances in Water Resources*, 76, 140–145. <https://doi.org/10.1016/j.advwatres.2014.11.012>
- Ford, T. W., & Labosier, C. F. (2017). Meteorological conditions associated with the onset of flash drought in the Eastern United States. *Agricultural and Forest Meteorology*, 247, 414–423. <https://doi.org/10.1016/j.agrformet.2017.08.031>
- Ford, T. W., McRoberts, D. B., Quiring, S. M., & Hall, R. E. (2015). On the utility of in situ soil moisture observations for flash drought early warning in Oklahoma, USA. *Geophysical Research Letters*, 42(22), 9790–9798. <https://doi.org/10.1002/2015gl066600>
- Gillespie, T. W., Ostermann-Kelm, S., Dong, C., Willis, K. S., Okin, G. S., & MacDonald, G. M. (2018). Monitoring changes of NDVI in protected areas of southern California. *Ecological Indicators*, 88, 485–494. <https://doi.org/10.1016/j.ecolind.2018.01.031>
- Goldberg, A., Panov, N., Gutman, G. G., Imhoff, M. L., Anderson, M., Pinker, R. T., et al. (2010). Use of NDVI and land surface temperature for drought assessment: Merits and limitations. *Journal of Climate*, 23(3), 618–633. <https://doi.org/10.1175/2009jcli2900.1>
- Griffin, D., & Anchukaitis, K. J. (2014). How unusual is the 2012–2014 California drought? *Geophysical Research Letters*, 41(24), 9017–9023. <https://doi.org/10.1002/2014gl062433>
- Griffith, G. E., Omernik, J. M., Smith, D. W., Cook, T. D., Tallyn, E., Moseley, K., & Johnson, C. B. (2016). Ecoregions of California (2016–1021). Retrieved from <http://pubs.er.usgs.gov/publication/ofr20161021>
- Gringorten, I. I. (1963). A plotting rule for extreme probability paper. *Journal of Geophysical Research*, 68(3), 813–814. <https://doi.org/10.1029/jz068i003p00813>
- Gu, Y., Brown, J. F., Verdin, J. P., & Wardlow, B. (2007). A five-year analysis of MODIS NDVI and NDWI for grassland drought assessment over the central Great Plains of the United States. *Geophysical Research Letters*, 34(6), L06407. <https://doi.org/10.1029/2006gl029127>
- Guo, H., Bao, A., Liu, T., Jiapaer, G., Ndayisaba, F., Jiang, L., et al. (2018). Spatial and temporal characteristics of droughts in Central Asia during 1966–2015. *Science of the Total Environment*, 624, 1523–1538. <https://doi.org/10.1016/j.scitotenv.2017.12.120>
- Guo, H., Bao, A., Ndayisaba, F., Liu, T., Jiapaer, G., El-Tantawi, A. M., & De Maeyer, P. (2018). Space-time characterization of drought events and their impacts on vegetation in Central Asia. *Journal of Hydrology*, 564, 1165–1178. <https://doi.org/10.1016/j.jhydrol.2018.07.081>
- Hao, Z., & AghaKouchak, A. (2013). Multivariate Standardized Drought Index: A parametric multi-index model. *Advances in Water Resources*, 57, 12–18. <https://doi.org/10.1016/j.advwatres.2013.03.009>
- Ho, S. Q.-G., Tian, L., Disse, M., & Tuo, Y. (2021). A new approach to quantify propagation time from meteorological to hydrological drought. *Journal of Hydrology*, 603, 127056. <https://doi.org/10.1016/j.jhydrol.2021.127056>
- Huang, S., Tang, L., Hupy, J. P., Wang, Y., & Shao, G. (2020). A commentary review on the use of normalized difference vegetation index (NDVI) in the era of popular remote sensing. *Journal of Forestry Research*, 32(1), 1–6. <https://doi.org/10.1007/s11676-020-01155-1>

- Ji, L., & Peters, A. J. (2003). Assessing vegetation response to drought in the northern Great Plains using vegetation and drought indices. *Remote Sensing of Environment*, 87(1), 85–98. [https://doi.org/10.1016/s0034-4257\(03\)00174-3](https://doi.org/10.1016/s0034-4257(03)00174-3)
- Le Houerou, H. (1996). Climate change, drought and desertification. *Journal of Arid Environments*, 34(2), 133–185. <https://doi.org/10.1006/jare.1996.0099>
- Li, J., Wang, Z., & Lai, C. (2020). Severe drought events inducing large decrease of net primary productivity in mainland China during 1982–2015. *Science of the Total Environment*, 703, 135541. <https://doi.org/10.1016/j.scitotenv.2019.135541>
- Li, J., Wang, Z., Wu, X., Chen, J., Guo, S., & Zhang, Z. (2020). A new framework for tracking flash drought events in space and time. *Catena*, 194, 104763. <https://doi.org/10.1016/j.catena.2020.104763>
- Li, W., Migliavacca, M., Forkel, M., Denissen, J. M. C., Reichstein, M., Yang, H., et al. (2022). Widespread increasing vegetation sensitivity to soil moisture. *Nature Communications*, 13(1), 3959. <https://doi.org/10.1038/s41467-022-31667-9>
- Lisonbee, J., Woloszyn, M., & Skumanich, M. (2021). Making sense of flash drought: Definitions, indicators, and where we go from here. *Journal of Applied and Service Climatology*, 2021(1), 1–19. <https://doi.org/10.46275/joasc.2021.02.001>
- Liu, Y., Zhu, Y., Ren, L., Otkin, J. A., Hunt, E. D., Yang, X., et al. (2020). Two different methods for flash drought identification: Comparison of their strengths and limitations. *Journal of Hydrometeorology*, 21(4), 691–704. <https://doi.org/10.1175/jhm-d-19-0088.1>
- Lloyd-Hughes, B. (2013). The impracticality of a universal drought definition. *Theoretical and Applied Climatology*, 117(3–4), 607–611. <https://doi.org/10.1007/s00704-013-1025-7>
- Lu, J., Carbone, G. J., Huang, X., Lackstrom, K., & Gao, P. (2020). Mapping the sensitivity of agriculture to drought and estimating the effect of irrigation in the United States, 1950–2016. *Agricultural and Forest Meteorology*, 292–293.
- Lund, J., Medellin-Azuara, J., Durand, J., & Stone, K. (2018). Lessons from California's 2012–2016 drought. *Journal of Water Resources Planning and Management*, 144(10). [https://doi.org/10.1061/\(asce\)wr.1943-5452.0000984](https://doi.org/10.1061/(asce)wr.1943-5452.0000984)
- Marston, L., & Konar, M. (2017). Drought impacts to water footprints and virtual water transfers of the Central Valley of California. *Water Resources Research*, 53(7), 5756–5773. <https://doi.org/10.1002/2016wr020251>
- McKee, T. B., Doesken, N. J., & McKee, J. K. (1993). The relationship of drought frequency and duration to time scales. In *Paper presented at the Eighth Conference on Applied Climatology* (Vol. 17).
- Mo, K. C., & Lettenmaier, D. P. (2015). Heat wave flash droughts in decline. *Geophysical Research Letters*, 42(8), 2823–2829. <https://doi.org/10.1002/2015gl064018>
- NASA-JPL. (2013). NASA shuttle radar topography mission global 1 arc second.
- Nguyen, H., Wheeler, M. C., Otkin, J. A., Cowan, T., Frost, A., & Stone, R. (2019). Using the evaporative stress index to monitor flash drought in Australia. *Environmental Research Letters*, 14(6), 064016. <https://doi.org/10.1088/1748-9326/ab2103>
- Nicolai-Shaw, N., Zscheischler, J., Hirschi, M., Gudmundsson, L., & Seneviratne, S. I. (2017). A drought event composite analysis using satellite remote-sensing based soil moisture. *Remote Sensing of Environment*, 203, 216–225. <https://doi.org/10.1016/j.rse.2017.06.014>
- Noguera, I., Domínguez-Castro, F., & Vicente-Serrano, S. M. (2021). Flash drought response to precipitation and atmospheric evaporative demand in Spain. *Atmosphere*, 12(2), 165. <https://doi.org/10.3390/atmos12020165>
- O, S., & Park, S. K. (2023). Flash drought drives rapid vegetation stress in arid regions in Europe. *Environmental Research Letters*, 18(1), 014028. <https://doi.org/10.1088/1748-9326/aca3a>
- Okin, G. S., Dong, C., Willis, K. S., Gillespie, T. W., & MacDonald, G. M. (2018). The impact of drought on native southern California vegetation: Remote sensing analysis using MODIS-derived time series. *Journal of Geophysical Research: Biogeosciences*, 123(6), 1927–1939. <https://doi.org/10.1029/2018jg004485>
- Orth, R., & Destouni, G. (2018). Drought reduces blue-water fluxes more strongly than green-water fluxes in Europe. *Nature Communications*, 9(1), 3602. <https://doi.org/10.1038/s41467-018-06013-7>
- Orth, R., Destouni, G., Jung, M., & Reichstein, M. (2020). Large-scale biospheric drought response intensifies linearly with drought duration in arid regions. *Biogeosciences*, 17(9), 2647–2656. <https://doi.org/10.5194/bg-17-2647-2020>
- Osman, M., Zaitchik, B. F., Badr, H. S., Christian, J. I., Tadesse, T., Otkin, J. A., & Anderson, M. C. (2021). Flash drought onset over the contiguous United States: Sensitivity of inventories and trends to quantitative definitions. *Hydrology and Earth System Sciences*, 25(2), 565–581. <https://doi.org/10.5194/hess-25-565-2021>
- Otkin, J. A., Svoboda, M., Hunt, E. D., Ford, T. W., Anderson, M. C., Hain, C., & Basara, J. B. (2018). Flash droughts: A review and assessment of the challenges imposed by rapid-onset droughts in the United States. *Bulletin of the American Meteorological Society*, 99(5), 911–919. <https://doi.org/10.1175/bams-d-17-0149.1>
- Otkin, J. A., Zhong, Y., Hunt, E. D., Basara, J., Svoboda, M., Anderson, M. C., & Hain, C. (2016). Assessing the evolution of soil moisture and vegetation conditions during a flash drought–flash recovery sequence over the South-Central United States. *Journal of Hydrometeorology*, 20(3), 549–562. <https://doi.org/10.1175/jhm-d-18-0171.1>
- Pauloo, R. A., Escrivá-Bou, A., Dahlke, H., Fencl, A., Guillon, H., & Fogg, G. E. (2020). Domestic well vulnerability to drought duration and unsustainable groundwater management in California's Central Valley. *Environmental Research Letters*, 15(4), 044010. <https://doi.org/10.1088/1748-9326/ab6f10>
- Pendergrass, A. G., Meehl, G. A., Pulwarty, R., Hobbins, M., Hoell, A., AghaKouchak, A., et al. (2020). Flash droughts present a new challenge for subseasonal-to-seasonal prediction. *Nature Climate Change*, 10(3), 191–199. <https://doi.org/10.1038/s41558-020-0709-0>
- Peng, C., Deng, M., & Di, L. (2014). Relationships between remote-sensing-based agricultural drought indicators and root zone soil moisture: A comparative study of Iowa. *Ieee Journal of Selected Topics in Applied Earth Observations and Remote Sensing*, 7(11), 4572–4580. <https://doi.org/10.1109/jstars.2014.2344115>
- Peng, J., Dadson, S., Hirpa, F., Dyer, E., Lees, T., Miralles, D. G., et al. (2020). A pan-African high-resolution drought index dataset. *Earth System Science Data*, 12(1), 753–769. <https://doi.org/10.5194/essd-12-753-2020>
- Peters, A. J., Walter-Shea, E. A., Ji, L., Vina, A., Hayes, M., & Svoboda, M. D. (2002). Drought monitoring with NDVI-based standardized vegetation index. *Photogrammetric Engineering & Remote Sensing*, 68(1), 71–75.
- Saxton, K. E., Rawls, W. J., Romberger, J. S., & Papendick, R. I. (1986). Estimating generalized soil-water characteristics from texture. *Soil Science Society of America Journal*, 50(4), 5. <https://doi.org/10.2136/sssaj1986.03615995005000040054x>
- Sheffield, J., Andreadis, K. M., Wood, E. F., & Lettenmaier, D. P. (2009). Global and continental drought in the second half of the twentieth century: Severity–area–duration analysis and temporal variability of large-scale events. *Journal of Climate*, 22(8), 1962–1981. <https://doi.org/10.1175/2008jcli2722.1>
- Spinoni, J., Barbosa, P., De Jager, A., McCormick, N., Naumann, G., Vogt, J. V., et al. (2019). A new global database of meteorological drought events from 1951 to 2016. *Journal of Hydrology: Regional Studies*, 22, 100593. <https://doi.org/10.1016/j.ejrh.2019.100593>
- Spruce, J. P., Gasser, G. E., & Hargrove, W. W. (2016). MODIS NDVI data, smoothed and gap-filled, for the Conterminous US: 2000–2015. <https://doi.org/10.3334/ORNLDAAC/1299>

- Stagge, J. H., Tallaksen, L. M., Gudmundsson, L., Van Loon, A. F., & Stahl, K. (2015). Candidate distributions for climatological drought indices (SPI and SPEI). *International Journal of Climatology*, *35*(13), 4027–4040. <https://doi.org/10.1002/joc.4267>
- Svoboda, M., LeComte, D., Hayes, M., Heim, R., Gleason, K., Angel, J., et al. (2002). The drought monitor. *Bulletin of the American Meteorological Society*, *83*(8), 1181–1190. <https://doi.org/10.1175/1520-0477-83.8.1181>
- Taylor, R. (1990). Interpretation of the correlation coefficient: A basic review. *Journal of Diagnostic Medical Sonography*, *6*(1), 35–39. <https://doi.org/10.1177/875647939000600106>
- Teluguntla, P., Thenkabail, P., Xiong, J., Gumma, M., Giri, C., Milesi, C., et al. (2015). Global food security support analysis data (GFSAD) at nominal 1 km (GCAD) derived from remote sensing in support of food security in the twenty-first century: Current achievements and future possibilities.
- Tucker, C. J. (1979). Red and photographic infrared linear combinations for monitoring vegetation. *Remote Sensing of Environment*, *8*(2), 127–150. [https://doi.org/10.1016/0034-4257\(79\)90013-0](https://doi.org/10.1016/0034-4257(79)90013-0)
- Vicente-Serrano, S. M., Gouveia, C., Camarero, J. J., Begueria, S., Trigo, R., Lopez-Moreno, J. I., et al. (2013). Response of vegetation to drought time-scales across global land biomes. *Proceedings of the National Academy of Sciences of the United States of America*, *110*(1), 52–57. <https://doi.org/10.1073/pnas.1207068110>
- Vicente-Serrano, S. M., Miralles, D. G., Domínguez-Castro, F., Azorin-Molina, C., El Kenawy, A., McVicar, T. R., et al. (2018). Global assessment of the standardized evapotranspiration deficit index (SEDI) for drought analysis and monitoring. *Journal of Climate*, *31*(14), 5371–5393. <https://doi.org/10.1175/jcli-d-17-0775.1>
- Walkinshaw, M., O'Geen, A. T., & Beaudette, D. E. (2022). Soil properties. Retrieved from casoilresource.lawr.ucdavis.edu/soil-properties/
- Wang, A., Lettenmaier, D. P., & Sheffield, J. (2011). Soil moisture drought in China, 1950–2006. *Journal of Climate*, *24*(13), 3257–3271. <https://doi.org/10.1175/2011jcli3733.1>
- Wang, L., & Yuan, X. (2018). Two types of flash drought and their connections with seasonal drought. *Advances in Atmospheric Sciences*, *35*(12), 1478–1490. <https://doi.org/10.1007/s00376-018-8047-0>
- Wilson, T. S., Sleeter, B. M., & Cameron, D. R. (2016). Future land-use related water demand in California. *Environmental Research Letters*, *11*(5), 054018. <https://doi.org/10.1088/1748-9326/11/5/054018>
- Xiao, M., Koppa, A., Mekonnen, Z., Pagán, B. R., Zhan, S., Cao, Q., et al. (2017). How much groundwater did California's Central Valley lose during the 2012–2016 drought? *Geophysical Research Letters*, *44*(10), 4872–4879. <https://doi.org/10.1002/2017gl073333>
- Xiao, X., Flanagan, P. X., Wakefield, R. A., Hunt, E. D., Otkin, J. A., Basara, J. B., & Christian, J. I. (2019). A methodology for flash drought identification: Application of flash drought frequency across the United States. *Journal of Hydrometeorology*, *20*(5), 833–846. <https://doi.org/10.1175/jhm-d-18-0198.1>
- Xu, K., Yang, D., Yang, H., Li, Z., Qin, Y., & Shen, Y. (2015). Spatio-temporal variation of drought in China during 1961–2012: A climatic perspective. *Journal of Hydrology*, *526*, 253–264. <https://doi.org/10.1016/j.jhydrol.2014.09.047>
- Xue, J., & Su, B. (2017). Significant remote sensing vegetation indices: A review of developments and applications. *Journal of Sensors*, *2017*, 1–17. <https://doi.org/10.1155/2017/1353691>
- Zang, C. S., Buras, A., Esquivel-Muelbert, A., Jump, A. S., Rigling, A., & Rammig, A. (2019). Standardized drought indices in ecological research: Why one size does not fit all. *Global Change Biology*, *26*(2), 322–324. <https://doi.org/10.1111/gcb.14809>
- Zhang, J., Guan, K., Peng, B., Pan, M., Zhou, W., Jiang, C., et al. (2021). Sustainable irrigation based on co-regulation of soil water supply and atmospheric evaporative demand. *Nature Communications*, *12*(1), 5549. <https://doi.org/10.1038/s41467-021-25254-7>
- Zhang, M., & Yuan, X. (2020). Rapid reduction in ecosystem productivity caused by flash droughts based on decade-long FLUXNET observations. *Hydrology and Earth System Sciences*, *24*(11), 5579–5593. <https://doi.org/10.5194/hess-24-5579-2020>
- Zomer, R. J., & Trabucco, A. (2022). Global Aridity Index and Potential Evapo-Transpiration Dataset v3.
- Zotarelli, L., Dukes, M. D., Romero, C. C., Migliaccio, K. W., & Morgan, K. T. (2010). *Step by step calculation of the Penman-Monteith evapotranspiration (FAO-56 method)*. Institute of Food and Agricultural Sciences, University of Florida.